

Article

# Hybrid Disila-Crown Ethers as Hosts for Ammonium Cations: The O–Si–Si–O Linkage as an Acceptor for Hydrogen Bonding

Fabian Dankert, Kirsten Reuter, Carsten Donsbach and Carsten von Hänisch \* 

Fachbereich Chemie and Wissenschaftliches Zentrum für Materialwissenschaften (WZMW), Philipps-Universität Marburg, Hans-Meerwein Straße 4, D-35032 Marburg, Germany; fabian.dankert@staff.uni-marburg.de (F.D.); kirsten.reuter@staff.uni-marburg.de (K.R.); donsbach@students.uni-marburg.de (C.D.)

\* Correspondence: haenisch@chemie.uni-marburg.de; Tel.: +49-06421-2825612

Received: 11 December 2017; Accepted: 11 January 2018; Published: 16 January 2018

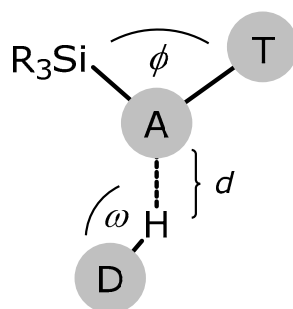
**Abstract:** Host-guest chemistry was performed with disilane-bearing crown ethers and the ammonium cation. Equimolar reactions of 1,2-disila[18]crown-6 (**1**) or 1,2-disila-benzo[18]crown-6 (**2**) and  $\text{NH}_4\text{PF}_6$  in dichloromethane yielded the respective compounds  $[\text{NH}_4(1,2\text{-disila}[18]\text{crown-6})]\text{PF}_6$  (**3**) and  $[\text{NH}_4(1,2\text{-disila-benzo}[18]\text{crown-6})]\text{PF}_6$  (**4**). According to X-ray crystallographic, NMR, and IR experiments, the uncommon hydrogen bonding motif  $\text{O}_{(\text{Si})}\cdots\text{H}$  could be observed and the use of cooperative effects of ethylene and disilane bridges as an effective way to incorporate guest molecules was illustrated.

**Keywords:** siloxanes; host-guest chemistry; supramolecular chemistry; main group coordination chemistry; hydrogen bonding

## 1. Introduction

Siloxane bonding has been intensely discussed for the past seventy years. However, siloxane bonding is not yet fully understood. Its discussion regarding the basicity is, to the best of our knowledge, nowadays based on two different explanatory models. Both are important in order to give insights into the Si–O bond, the associated Lewis basicity, and binding properties. As one model, negative hyperconjugation interactions are discussed especially for permethylated siloxanes [1,2]. These interactions are understood as a donation of electron density in the case  $p(\text{O}) \rightarrow \sigma^*(\text{Si}-\text{C})$ , which is competing with the coordination towards a Lewis acid and vice versa. Hence, the basicity of silicon bonded oxygen atoms turns out to be lower [3–5]. The other explanatory model considers the Si–O bond as highly ionic. The electronegativity gradient in the Si–O bond is considerably larger than in the C–O bond, which causes significantly different binding properties of siloxanes in comparison to ethers. Gillespie and Robinson emphasize that the electron pairs located directly at the oxygen atoms are spatially diffused, resulting in a lower basicity [6]. Furthermore, one could argue that the partially negatively charged oxygen atoms should show strong interactions with Lewis acids. However, this argument is disproved by repulsive interactions between a positively charged silicon atom and a Lewis acid, which was recently shown via quantum chemical calculations [7,8]. Overall, this leads to an understanding of why the coordination of siloxanes turns out to be cumbersome. The whole discussion is stripped down to monosilanes, which results in a structural discrepancy regarding (cyclic) poly-silaethers. The conformation of the ligand significantly affects the coordination properties, which was shown for ring-contracted crown ethers [9,10]. Considering all those arguments, we tried to regain structural analogy towards organic (crown type) ligands with the insertion of disilane-units. Simple substitution of  $-\text{SiMe}_2-$  units with  $-\text{Si}_2\text{Me}_4-$  units in a residuary  $-\text{C}_2\text{H}_4\text{O}-$  framework yields

disilane-bearing ligands with a respectable coordination ability very close to their organic analogs. Alkali and alkaline earth metal salts could easily be coordinated by ligands of this class, so the coordination ability of siloxane compounds should be reconsidered [11–15]. However, the discussion around siloxane bonding is not restricted to the coordination of Lewis acids and includes the ability to form hydrogen bonds. Hydrogen-bonding patterns vary with the use of different substituents within a silicon-based system (see Scheme 1).



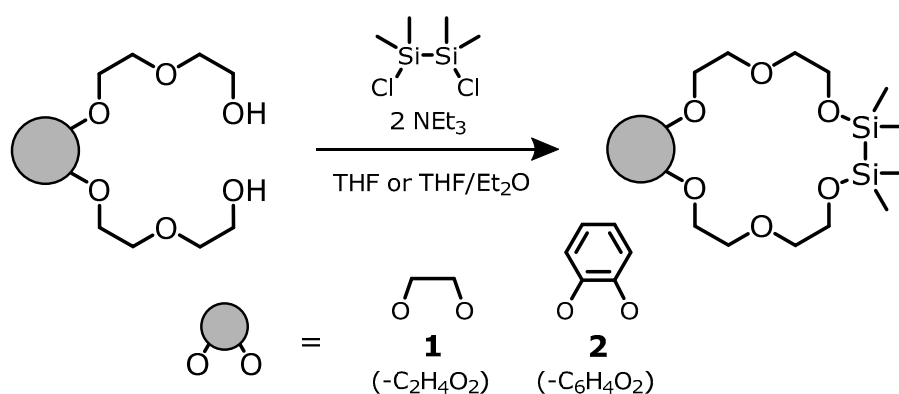
**Scheme 1.** Model of hydrogen-bonding involving silicon-based systems in which A = acceptor (especially O), D = donor-bearing atom (O/N), T = tetrel (C/Si),  $d$  = length of the respective hydrogen bonding contact, and  $\phi$  as well as  $\omega$  are relevant bond angles setting up the hydrogen bonding pattern.

The ability of these systems to form a hydrogen bond has been discussed since the early sixties, especially by the group of West. Early examinations order the affinity to form hydrogen bonds in the sequence  $R_3COCR_3 > R_3COSiR_3 \gg R_3SiOSiR_3$  according to IR-spectroscopic and thermodynamic studies, as well as NMR experiments [16–18]. Also, recent research confirms a low hydrogen bonding affinity of the oxygen atoms within ligands of the type  $R_3SiOSiR_3$  [19]. This is also reflected by the fact that a lot more solid state structures with hydrogen bonding between D–H and  $R_3CDSiR_3$  (D = O, N) than between D–H and  $R_3SiOSiR_3$  are known to date. These results reflect the fact that a screening of the Cambridge Crystallographic Database (CCDC) reveals no more than twenty structures that exhibit hydrogen bonding between D–H and  $R_3CDSiR_3$  (D = O, N) and just a handful of structures showing contacts in between D–H and  $R_3SiOSiR_3$  in the solid state [20]. Taking all observations into account, the hydrogen bonding of siloxanes continues to be an uncommon motif and is declared as an unusual phenomenon [21]. However, it is possible to increase the ability of siloxanes to form hydrogen bonds by decreasing the  $\phi$ -angle, which could be shown in several publications and was also supported by experimental data provided by the group of Beckmann [5,17,21–23]. The relatively small pool of experimental data motivated us to extend the coordination chemistry of hybrid disila-crown ethers to ammonium cations.

## 2. Results

The ability of organic crown ethers to act as host molecules is discussed regarding different systems with hydronium- and ammonium ions as the simplest hosts. Recrystallization of equimolar ratios of salt and an appropriate crown ether from organic and/or aqueous solution yields crown ether complexes with the general formula  $[M(CE)]A$ , where  $M = H_3O^+$  or  $NH_4^+$ , CE = crown ether, and A = anion. Mainly crown ethers of the [18]crown-6 type are used, but the anion structure varies with  $A = Cl^-, Br_3^-, I_3^-, ClO_4^-, [BF_4]^- , [PF_6]^- [SbCl_6]^-$ , and many more [24–33]. In the case of hybrid crown-ethers, aqueous solutions and traces of moisture lead to the entire decomposition of the ligand. Siloxane cleavage with aqueous solutions is common for this kind of ligand and has already been discussed in other publications [11,34,35]. For this reason, hydrogen bonding towards hydronium cations could not be performed. However, the incorporation of a guest turned out to be successful in the use of ammonium hexafluorophosphate as the salt and 1,2-disila[18]crown-6 (**1**), as well as 1,2-disila-benzo[18]crown-6 (**2**) as the ligands of choice. The ligands were prepared using methods

described in the literature (see Scheme 2) [11,15]. Subsequent reaction of these ligands with  $\text{NH}_4\text{PF}_6$  in anhydrous dichloromethane yielded the respective complexes  $[\text{NH}_4(1,2\text{-disila}[18]\text{crown-6})\text{PF}_6]$  (**3**) and  $[\text{NH}_4(1,2\text{-disila-benzo}[18]\text{crown-6})\text{PF}_6]$  (**4**). Neat **3** is a colorless powder which can be recrystallized from dichloromethane. The resulting colorless blocks were analyzed via XRD. **3** crystallizes in the non-centrosymmetric monoclinic space group  $P2_1$  as an enantiopure product very similar to the corresponding potassium complex  $[\text{K}(1,2\text{-disila}[18]\text{crown-6})\text{PF}_6]$  according to the lattice constants [11]. As also observed for organic crown ether complexes, the ammonium cation is trapped in the cavity of the sila-crown ether beneath the anion bound to every second oxygen atom of the ligand **1**. The hydrogen bonding system of the ammonium cation now features three different binding modes due to the insertion of the O–Si–Si–O linkage and the presence of the  $[\text{PF}_6]^-$  anion. Hence, etheric oxygen atoms, one silicon substituted oxygen atom, and two of the fluorine atoms of the  $[\text{PF}_6]^-$  anion are participating (see Figure 1). The F...H contacts show distances that are well within the range of hydrogen bonding for this system. Freely chosen systems for comparison are  $[\text{NH}_4([\text{18}]\text{crown-6})\text{PF}_6]$ ,  $[\text{NH}_4(\text{dibenzo}[18]\text{crown-6})\text{PF}_6]$ , and  $[\text{NH}_4(\text{benzo}[15]\text{crown-5})\text{PF}_6]$  [32,36,37].



**Scheme 2.** Synthesis of 1,2-disila[18]crown-6 and 1,2-disila-benzo[18]crown-6 [11,15].

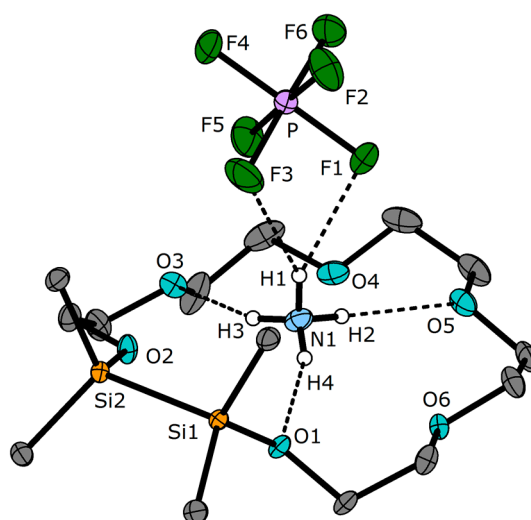


**Figure 1.** The molecular structure of compound **3** in the solid state. Thermal ellipsoids represent a probability level of 50%. The disordered part of the ligand with a lower occupancy and all carbon bonded hydrogen atoms are omitted for clarity, whereas hydrogen atoms of the ammonium cation are represented with arbitrary atomic radii. The latter were refined with DFIX [0.91] commands. Selected contacts and bond lengths [pm]: H1...F1 222(3), H1...F2 236(3), H2...O5 206(3), H3...O3 203(6), H4...O1 205(3), Si1–Si2 234.8(1).

Compound **3** is a rare example combining hydrogen bonding situations towards etheric oxygen atoms, as well as partially silicon substituted oxygen atoms in the same molecule. This enables a comparative analysis of the respective hydrogen bond donating properties of the different oxygen atoms. The hydrogen bonding data for **3** and related compounds-based on the representation in Scheme 1 are presented in Table 1. The respective hydrogen bonding patterns of **3** show no significant divergence between the  $O_{(organic)}\cdots H$  and  $O_{(Si)}\cdots H$  contacts. Hence, there is no hint of a preference of the etheric oxygen atoms to form hydrogen bonding. The N–H4 $\cdots$ O1 contact has a rather short value of 205 pm, but is still in agreement with those in the related compounds. So, it can be assumed that the use of cooperative effects of ether and disilane bridges seems to be an effective way to incorporate guest molecules.

**Table 1.** Hydrogen bonding geometry in **3**, **4**, and related silicon based systems.

Compound or CSD Refcode <sup>1</sup>	D–H <sup>2</sup>	A	<i>d</i> [pm]	T <sup>3</sup>	$\omega$ [°]	$\phi$ [°]	Ref. <sup>4</sup>
<b>3</b>	N–H2	O5	206	C <sub>E</sub>	160	113	*
	N–H3	O3	203	C <sub>E</sub>	156	108	*
	N–H4	O1	205	C	159	122	*
<b>4</b>	N–H2	O4	214	C <sub>E</sub>	165	117	*
	N–H3	O2	209	C <sub>E</sub>	151	110	*
	N–H4	O6	200	C	172	118	*
VONMOB	N–H	O	226	C	174	128	[38]
MEQFOD	N–H	O	247	C	141	131	[39]
ITUBUI	N–H	O	198–210	C	157–160	130–132	[40]
MOLYUO	O–H	O	192	Si	167	116	[23]
TAKFOB	O–H	O	257–260	Si	148–152	139–148	[41]
ZEMXAQ	O–H	O	199	Si	156	116	[42]
EGEKAC	O–H	O	199–200	C	155–161	114–115	[43]
PERWIS	O–H	O	199	C	166	123	[44]
REXXAT	O–H	O	199	C	173	111	[45]

<sup>1</sup> Choice of CSD Codes is based on ref. [20]. Geometric criteria for the search were similar to those in ref [21]. CCDC ConQuest Version 1.19 was used for the search; <sup>2</sup> See Scheme 1 for abbreviations; <sup>3</sup> Subscript E denotes that the hydrogen bonding refers to an etheric oxygen atom: two carbon atoms are located next to one oxygen atom; <sup>4</sup> \* = published within this work.

The successful incorporation of the ammonium cation in the silicon containing [18]crown-6 ether and its interesting bonding relations prompted us to synthesize another ammonium complex using the similar ligand **2**. Thereby, we obtained compound **4** as a white powder, which was further recrystallized from a mixture of dichloromethane and cyclopentane, yielding colorless rods suitable for single crystal X-ray diffraction analysis (see Figure 2 and Table 2). **4** crystallizes in the monoclinic space group *Cc* and reveals a trapped ammonium cation in the middle of the crown ether cavity bound to every second oxygen atom of the ligand **2**. The [PF<sub>6</sub>]<sup>−</sup> anion and one molecule of co-crystalline DCM are located above and beneath the ammonium cation. In comparison to compound **3**, the ammonium cation is located closer to the calculated mean plane spanned by the donor atoms of the crown ether with 45 pm in the case of **4** and 59 pm in the case of **3**. The hydrogen bonding geometry of **4** is slightly different to that of **3** because of the rather rigid, *ortho*-bridging phenyl unit (see Table 1). Similar to the  $O_{(organic)}\cdots H$  and  $O_{(Si)}\cdots H$  in **3**, the respective hydrogen bonding contacts show no significant divergence. However, due to the incorporation of co-crystalline DCM, an intrinsic disorder causes problems with the crystal structure refinement. For this reason, several restraints on distances and anisotropic displacement parameters were used during the refinement. Hence, the hydrogen-bonding situation between the ligand and ammonium cation should be considered carefully and is not discussed in detail as done for **3**. Recrystallization attempts from other solvents failed. Nonetheless, the crystal structure clearly indicates the participation of the silicon bonded oxygen atom regarding hydrogen bonding.

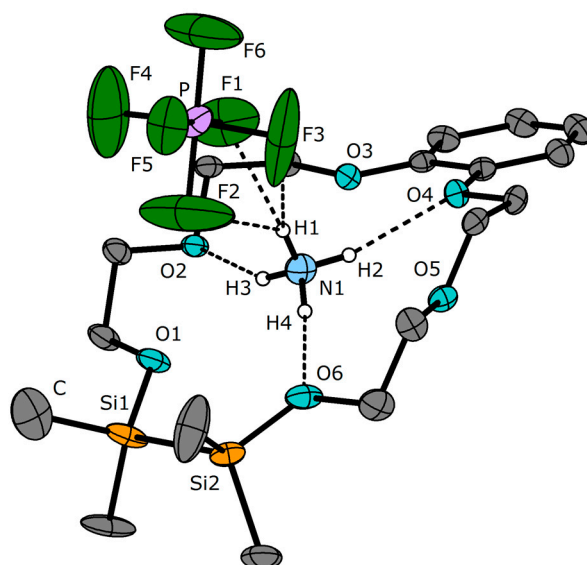


**Figure 2.** The molecular structure of compound **4** in the solid state. Thermal ellipsoids represent a probability level of 50%. The disordered part of the ligand with a lower occupancy and all carbon bonded hydrogen atoms, as well as the DCM molecule, are omitted for clarity. The hydrogen atoms of the ammonium cation are represented with arbitrary atomic radii. The latter were refined with DFIX [0.91] commands. Selected contacts and bond lengths [pm]: H1...F1 212(4) pm, H1...F2 247(5), H1...F3 279(5), H2...O4 213(6), H3...O2 209(5), H4...O6 200(3), Si1–Si2 233.9(3).

**Table 2.** X-ray crystallographic data for compounds **3** and **4·DCM**.

	<b>3</b>	<b>4·DCM</b>
Empirical formula	C <sub>14</sub> H <sub>36</sub> F <sub>6</sub> NO <sub>6</sub> PSi <sub>2</sub>	C <sub>19</sub> H <sub>38</sub> Cl <sub>2</sub> F <sub>6</sub> NO <sub>6</sub> PSi <sub>2</sub>
Formula weight [g·mol <sup>−1</sup> ]	515.59	648.55
Crystal colour, shape	colourless block	colourless rod
Crystal size [mm]	0.487 × 0.432 × 0.346	0.076 × 0.106 × 0.522
Crystal system	monoclinic	monoclinic
Space group	<i>P</i> 2 <sub>1</sub>	<i>C</i> c
Formula units	2	4
Temperature [K]	100(2)	100(2)
Unit cell dimensions [Å, °]	<i>a</i> = 10.4542(5) <i>b</i> = 12.3869(6) <i>c</i> = 10.6140(5) <i>β</i> = 117.912(1)	<i>a</i> = 14.9582(7) <i>b</i> = 12.6454(6) <i>c</i> = 16.3325(8) <i>β</i> = 104.950(2)
Cell volume [Å <sup>3</sup> ]	1214.57(10)	2984.8(2)
<i>ρ</i> calc [g/cm <sup>3</sup> ]	1.410	1.443
<i>μ</i> [mm <sup>−1</sup> ]	0.286	0.422
2 $\theta$ range [°]	4.342 to 50.568	4.280 to 53.570
Reflections measured	34532	68974
Independent reflections	4419	6355
<i>R</i> <sub>1</sub> ( <i>I</i> > 2 $\sigma$ ( <i>I</i> ))	0.0203	0.0535
<i>wR</i> <sub>2</sub> (all data)	0.0529	0.1329
Goof	1.076	1.035
Largest diff. peak/hole [e·Å <sup>−3</sup> ]	0.24/−0.27	0.51/−0.44
Flack parameter	0.004(14)	0.048(16)

The interactions between the silicon affected oxygen atoms and the hydrogen atoms of the ammonium cation are further verified by NMR and IR experiments. As observed for the metal complexes of disila-crown ethers, a characteristic downfield shift of the singlet in the <sup>29</sup>Si{<sup>1</sup>H} and the

singlet of the SiMe<sub>2</sub>-groups in the <sup>1</sup>H NMR spectra is observed for both compounds **3** and **4**. The <sup>29</sup>Si NMR shift is 13.7 ppm in the case of **3** and 16.2 ppm in the case of **4**. For this reason, both compounds show a dynamic process regarding the H-bonding situation. Rapid exchange results in the described equivalency of the silicon atoms. Even in VT NMR experiments, subsequently cooling the solution to 190 K did not result in an inequivalence of the SiMe<sub>2</sub> groups. The respective NMR shifts are in the range of sodium and potassium metal ion complexes of disila-crown ethers [11,14].

The <sup>1</sup>H NMR spectra represent the singlets for the SiMe<sub>2</sub> groups at 0.29 (**3**) and 0.30 (**4**) ppm, respectively. For the ammonium cations, triplets were observed at 6.44 ppm for **3** and at 6.64 ppm for **4** in the <sup>1</sup>H NMR spectra. As mentioned above, IR spectroscopic data also indicate an interaction of the ammonium cation with the silicon bonded oxygen atom. In comparison to pure NH<sub>4</sub>PF<sub>6</sub>, three instead of only one NH stretching vibrations are observed in both compounds. The respective signals are found at 3333 cm<sup>-1</sup> in NH<sub>4</sub>PF<sub>6</sub>; 3317, 3188, and 3086 cm<sup>-1</sup> in **3**; and 3298, 3225, and 3066 cm<sup>-1</sup> in **4**, comprising a significant red-shift in the coordinated cases [46]. This is in accordance with the solid-state structures found upon single crystal X-ray diffraction analysis, as three different binding modes of the NH<sub>4</sub>-related hydrogen atoms are revealed.

### 3. Materials and Methods

#### 3.1. Laboratory Procedures and Techniques

All working procedures were performed by the use of Schlenk techniques under Ar gas. Solvents were dried and freshly distilled before use. Ammonium hexafluorophosphate was stored and handled under Ar atmosphere using a glovebox of MBRAUN-type. NMR spectra were recorded on a Bruker AV III HD 300 MHz or AV III 500 MHz spectrometer (Bruker, Ettlingen, Germany), respectively. The MestReNova package was used for analyzation [47]. Infrared (IR) spectra of the respective samples were measured using attenuated total reflectance (ATR) mode on a Bruker Model Alpha FT-IR (Bruker, Billerica, MA, USA) stored in the glove box. OPUS-software package was applied throughout [48]. ESI-MS spectrometry was performed with an LTQ-FT (Waltham, MA, USA) and LIFDI-MS with an AccuTOF-GC device (Akishima, Tokyo, Japan). Elemental analysis data cannot be provided due to the presence of fluorine in the samples, which harms the elemental analysis devices.

#### 3.2. Crystal Structures

Single crystal X-ray experiments were carried out using a Bruker D8 Quest diffractometer (Bruker, Billerica, MA, USA) at 100(2) K with Mo K $\alpha$  radiation and X-ray optics ( $\lambda = 0.71073$ ). All structures were solved by direct methods and refinement with full-matrix-least-squares against  $F^2$  using *SHELXT*- and *SHELXL*-2015 on the OLEX2 platform. Crystallographic data for compounds **3** and **4** are denoted as follows: CCDC Nos. 1589283 (**3**), 1589284 (**4**-DCM) [49–51]. Crystallographic information files (CIF, see Supplementary Materials) can be obtained free of charge from the Cambridge Crystallographic Data Centre (CCDC) (link: [www.ccdc.cam.ac.uk/data\\_request/cif](http://www.ccdc.cam.ac.uk/data_request/cif)). Visualization of all structures was performed with Diamond software package Version 4.4.0 [52]. Thermal Ellipsoids are drawn at the 50% probability level.

#### 3.3. Experimental Section

The sila-crown ethers 1,2-disila[18]crown-6 (**1**) and 1,2-disila-benzo[18]crown-6 (**2**) were synthesized according to methods reported in literature [11,15]. Compounds **3** and **4** were synthesized as follows.

[NH<sub>4</sub>(1,2-disila[18]crown-6)]PF<sub>6</sub> (**3**): 106 mg of **1** (0.30 mmol, 1.0 eq) was dissolved in 15 mL of dichloromethane. A total of 59 mg of NH<sub>4</sub>PF<sub>6</sub> (1.2 eq, 0.36 mmol) was then added. Stirring the suspension for 72 h gave a cloudy solution, which was filtered followed by the removal of the solvent under reduced pressure. The raw product was washed with 5 mL of *n*-pentane and dried in vacuo. A total of 147 mg of **3** was obtained as a pale white powder in 94% yield. For single crystal growth,

**3** was dissolved in dichloromethane and the solvent was removed until saturation of the solution. Cooling to  $-32\text{ }^{\circ}\text{C}$  yielded colorless blocks after a few days.  $^1\text{H}$  NMR: (300 MHz,  $\text{CD}_2\text{Cl}_2$ )  $\delta = 0.29$  (s, 12H,  $\text{Si}(\text{CH}_3)_2$ ), 3.55–3.88 (m, 4H,  $\text{CH}_2$ ), 3.64 (s, 12H,  $\text{CH}_2$ ), 3.74–3.76 (m, 4H,  $\text{CH}_2$ ), 6.44 (t,  $^1J_{\text{NH}} = 54$  Hz, 4H,  $\text{NH}_4$ ) ppm;  $^{13}\text{C}\{^1\text{H}\}$  NMR: (75 MHz,  $\text{CD}_2\text{Cl}_2$ )  $\delta = -1.2$  (s,  $\text{Si}(\text{CH}_3)_2$ ), 62.9 (s,  $\text{CH}_2$ ), 70.7 (s,  $\text{CH}_2$ ), 70.8 (s,  $\text{CH}_2$ ), 70.9 (s,  $\text{CH}_2$ ), 72.9 (s,  $\text{CH}_2$ ) ppm;  $^{19}\text{F}$  NMR: (283 MHz)  $\delta = -72.5$  (d,  $^1J_{\text{PF}} = 713$  Hz,  $\text{PF}_6$ ) ppm;  $^{29}\text{Si}\{^1\text{H}\}$  NMR: (99 MHz,  $\text{CD}_2\text{Cl}_2$ )  $\delta = 13.7$  (s,  $\text{Si}(\text{CH}_3)_2$ ) ppm;  $^{31}\text{P}$  NMR: (203 MHz,  $\text{CD}_2\text{Cl}_2$ )  $\delta = -140.3$  (hept,  $^1J_{\text{PF}} = 713$  Hz,  $\text{PF}_6$ ) ppm. MS: LIFDI(+)  $m/z$  (%): 370.20784 [ $\text{M}-\text{PF}_6$ ] $^+$  (100), IR ( $\text{cm}^{-1}$ ): 3317 + 3188 + 3086 (m, br,  $\tilde{\nu}_s$  N–H), 2891 (m), 1453 (m), 1425.98 (m), 1352 (w), 1249 (m), 1097 (s), 1075 (s), 1060 (s), 953 (s) 920 (s), 830 (vs), 791 (vs), 769 (s), 739 (s), 713 (s), 626 (m), 556 (s), 518 (w).

$[\text{NH}_4(1,2\text{-disila-benzo}[18]\text{crown-6})]\text{PF}_6$  (**4**): 140 mg of **2** (0.35 mmol, 1.0 eq) was dissolved in 10 mL of Dichloromethane. Subsequent addition of 69 mg of  $\text{NH}_4\text{PF}_6$  (0.35 mmol, 1.0 eq) and stirring of the suspension for three hours yielded a clear solution that was subsequently freed of the solvent. The raw product was well washed with 8 mL of *n*-pentane, followed by drying in vacuo. A total of 200 mg of **4** was obtained as a pale white powder in 95% yield. For single crystal growth, **4** was dissolved in 2 mL of dichloromethane, layered with 15 mL cyclopentane, and finally stored at  $-32\text{ }^{\circ}\text{C}$  to obtain colorless rods after a few days.  $^1\text{H}$  NMR: (300 MHz,  $\text{CD}_2\text{Cl}_2$ )  $\delta = 0.30$  (s, 12H,  $\text{Si}(\text{CH}_3)_2$ ), 3.63–3.71 (m, 4H,  $\text{CH}_2$ ), 3.74–3.83 (m, 4H,  $\text{CH}_2$ ), 3.85–3.95 (m, 4H,  $\text{CH}_2$ ), 4.15–4.23 (m, 4H,  $\text{CH}_2$ ), 6.64 (t,  $^1J_{\text{NH}} = 54$  Hz, 4H,  $\text{NH}_4$ ) ppm; 6.86–7.04 (m, 4H,  $\text{C}_6\text{H}_4$ ).  $^{13}\text{C}\{^1\text{H}\}$  NMR: (75 MHz,  $\text{CD}_2\text{Cl}_2$ )  $\delta = 2.5$  (s,  $\text{Si}(\text{CH}_3)_2$ ), 62.02 (s,  $\text{CH}_2$ ), 68.6 (s,  $\text{CH}_2$ ), 69.6 (s,  $\text{CH}_2$ ), 72.8 (s,  $\text{CH}_2$ ), 113.6 (s,  $\text{C}_{\text{Ar,H}}$ ), 122.4 (s,  $\text{C}_{\text{Ar,H}}$ ), 148.3 (s,  $\text{C}_{\text{Ar,q}}$ ) ppm;  $^{19}\text{F}$  NMR: (283 MHz)  $\delta = -72.9$  (d,  $^1J_{\text{PF}} = 712$  Hz,  $\text{PF}_6$ ) ppm;  $^{29}\text{Si}\{^1\text{H}\}$  NMR: (99 MHz,  $\text{CD}_2\text{Cl}_2$ )  $\delta = 16.2$  (s,  $\text{Si}(\text{CH}_3)_2$ ) ppm;  $^{31}\text{P}$  NMR (203 MHz,  $\text{CD}_2\text{Cl}_2$ ):  $-143.8$  (hept,  $^1J_{\text{PF}} = 713$  Hz,  $\text{PF}_6$ ) ppm. MS: ESI(+)  $m/z$  (%): 418.2080 [ $\text{M}-\text{PF}_6$ ] $^+$  (100), IR ( $\text{cm}^{-1}$ ): 3298, 3225, 3066 (m, br,  $\tilde{\nu}_s$  N–H), 2946 (m), 2878 (m), 1594 (w), 1505 (m), 1454 (m), 1425 (m), 1249 (s), 1209 (s), 1121 (m) 1069 (s), 957 (m), 830 (vs), 791 (vs), 765 (vs), 738 (vs), 632 (w), 555 (vs).

#### 4. Conclusions

In this work, the incorporation of guest molecules into disilane-bearing crown ethers was discussed. The complexation of ammonium cations by the ligands **1** and **2** turned out to be successful. Within the respective complexes **3** and **4**, H-bonding between a silicon affected oxygen atom and the ammonium cation was purposefully realized. So far, related H-bonding was only observed as an occasional occurrence in solid-state structures. In addition,  $\text{O}_{(\text{organic})}\cdots\text{H}$  and  $\text{O}_{(\text{Si})}\cdots\text{H}$  contacts show no significant divergence on a structural level. Hence, there is no hint for a preference of the etheric oxygen atoms to form hydrogen bonding. The interaction of the protons related to the ammonium cation with the silicon affected oxygen atoms was verified by NMR- and IR-spectroscopic experiments. It can be concluded that the use of cooperative effects of ethylene and disilane bridges is an effective way to incorporate guest molecules. We are currently aiming for the synthesis of all-disilane substituted crown ether analogs. Systems of the type  $\text{SiSi-O-SiSi}$  will help advance our understanding of the siloxane linkage in combination with hydrogen bonding.

**Supplementary Materials:** The following are available online at [www.mdpi.com/2304-6740/6/1/15/s1](http://www.mdpi.com/2304-6740/6/1/15/s1), Cif and cif-checked files.

**Acknowledgments:** This work was financially supported by the Deutsche Forschungsgemeinschaft (DFG). Fabian Dankert gratefully acknowledges the kind advice and meticulous data collection of Michael Marsch (X-ray department, Philipps-University Marburg). Fabian Dankert further thanks N. Mais for his help with synthetic work.

**Author Contributions:** Fabian Dankert performed the synthesis and analytics of compound **4**, interpretations of all the analytical data, contributed to the X-ray crystallographic refinement, and wrote the manuscript. Kirsten Reuter performed the synthesis of compound **3** and the collection of the respective analytical data. Carsten Donsbach accomplished the crystal structure solution and refinement of compound **4**. Carsten von Hänisch contributed to the interpretation and manuscript preparation and led the overarching research project.

**Conflicts of Interest:** The authors declare no conflict of interest.

## References

1. Weinhold, F.; West, R. The nature of the silicon–oxygen bond. *Organometallics* **2011**, *30*, 5815–5824. [[CrossRef](#)]
2. Weinhold, F.; West, R. Hyperconjugative Interactions in Permethylated Siloxanes and Ethers: The Nature of the SiO Bond. *J. Am. Chem. Soc.* **2013**, *135*, 5762–5767. [[CrossRef](#)] [[PubMed](#)]
3. Ritch, J.S.; Chivers, T. Siliciumanaloga von Kronenethern und Cryptanden: Ein neues Kapitel in der Wirt-Gast-Chemie? *Angew. Chem.* **2007**, *119*, 4694–4697. [[CrossRef](#)]
4. Shambayati, S.; Blake, J.F.; Wierschke, S.G.; Jorgensen, W.L.; Schreiber, S.L. Structure and Basicity of Silyl Ethers: A Crystallographic and ab Initio Inquiry into the Nature of Silicon–Oxygen Interactions. *J. Am. Chem. Soc.* **1990**, *112*, 697–703. [[CrossRef](#)]
5. Cypryk, M.; Apeloig, Y. Ab Initio Study of Silyloxonium Ions. *Organometallics* **1997**, *16*, 5938–5949. [[CrossRef](#)]
6. Gillespie, R.J.; Robinson, E. Models of molecular geometry. *Chem. Soc. Rev.* **2005**, *34*, 396–407. [[CrossRef](#)] [[PubMed](#)]
7. Passmore, J.; Rautiainen, J.M. On The Lower Lewis Basicity of Siloxanes Compared to Ethers. *Eur. J. Inorg. Chem.* **2012**, *2012*, 6002–6010. [[CrossRef](#)]
8. Cameron, T.S.; Decken, A.; Krossing, I.; Passmore, J.; Rautiainen, J.M.; Wang, X.; Zeng, X. Reactions of a Cyclodimethylsiloxane (Me<sub>2</sub>SiO)<sub>6</sub> with Silver Salts of Weakly Coordinating Anions; Crystal Structures of [Ag(Me<sub>2</sub>SiO)<sub>6</sub>][Al] ([Al] = [Al{OC(CF<sub>3</sub>)<sub>3</sub>}<sub>3</sub>]<sub>3</sub>, [Al{OC(CF<sub>3</sub>)<sub>3</sub>}<sub>4</sub>]) and Their Comparison with [Ag(18-Crown-6)]<sub>2</sub>[SbF<sub>6</sub>]<sub>2</sub>. *Inorg. Chem.* **2013**, *52*, 3113–3126. [[CrossRef](#)] [[PubMed](#)]
9. Ouchi, M.; Inoue, Y.; Kanzaki, T.; Hakushi, T. Ring-contracted Crown Ethers: 14-Crown-5, 17-Crown-6, and Their Sila-analogues. Drastic Decrease in Cation-binding Ability. *Bull. Chem. Soc. Jpn.* **1984**, *57*, 887–888. [[CrossRef](#)]
10. Inoue, Y.; Ouchi, M.; Hakushi, T. Molecular Design of Crown Ethers. 3. Extraction of Alkaline Earth and Heavy Metal Picrates with 14- to 17-Crown-5 and 17- to 22-Crown-6. *Bull. Chem. Soc. Jpn.* **1985**, *58*, 525–530. [[CrossRef](#)]
11. Reuter, K.; Buchner, M.R.; Thiele, G.; von Hänisch, C. Stable Alkali-Metal Complexes of Hybrid Disila-Crown Ethers. *Inorg. Chem.* **2016**, *55*, 4441–4447. [[CrossRef](#)] [[PubMed](#)]
12. Reuter, K.; Thiele, G.; Hafner, T.; Uhlig, F.; von Hänisch, C. Synthesis and coordination ability of a partially silicon based crown ether. *Chem. Commun.* **2016**, *52*, 13265–13268. [[CrossRef](#)] [[PubMed](#)]
13. Reuter, K.; Rudel, S.S.; Buchner, M.R.; Kraus, F.; von Hänisch, C. Crown ether complexes of alkali metal chlorides from SO<sub>2</sub>. *Chem. Eur. J.* **2017**, *23*, 9607–9617. [[CrossRef](#)] [[PubMed](#)]
14. Reuter, K.; Dankert, F.; Donsbach, C.; von Hänisch, C. Structural Study of Mismatched Disila-Crown Ether Complexes. *Inorganics* **2017**, *5*, 11. [[CrossRef](#)]
15. Dankert, F.; Reuter, K.; Donsbach, C.; von Hänisch, C. A structural study of alkaline earth metal complexes with hybrid disila-crown ethers. *Dalton Trans.* **2017**, *46*, 8727–8735. [[CrossRef](#)] [[PubMed](#)]
16. West, R.; Whatley, L.S.; Lake, K.J. Hydrogen Bonding Studies. V. The Relative Basicities of Ethers, Alkoxysilanes and Siloxanes and the Nature of the Silicon–Oxygen Bond. *J. Am. Chem. Soc.* **1961**, *83*, 761–764. [[CrossRef](#)]
17. West, R.; Wilson, L.S.; Powell, D.L. Basicity of siloxanes, alkoxysilanes and ethers toward hydrogen bonding. *J. Organomet. Chem.* **1979**, *178*, 5–9. [[CrossRef](#)]
18. Popowski, E.; Schulz, J.; Feist, K.; Kelling, H.; Jancke, H. Basizität und <sup>29</sup>Si-NMR-spektroskopische Untersuchungen von Ethoxysiloxanen. *Z. Anorg. Allg. Chem.* **1988**, *558*, 206–216. [[CrossRef](#)]
19. Yilgör, E.; Burgaz, E.; Yurtsever, E.; Yilgör, I. Comparison of hydrogen bonding in polydimethylsiloxane and polyether based urethane and urea copolymers. *Polymer* **2000**, *41*, 849–857. [[CrossRef](#)]
20. Jeffrey, G.A. *An Introduction to Hydrogen Bonding*; Oxford University Press: Oxford, UK, 1997.
21. Grabowsky, S.; Beckmann, J.; Luger, P. The Nature of Hydrogen Bonding Involving the Siloxane Group. *Aust. J. Chem.* **2012**, *65*, 785–795. [[CrossRef](#)]
22. Frolov, Y.L.; Voronkov, M.G.; Strashnikova, N.V.; Shergina, N.I. Hydrogen bonding involving the siloxane group. *J. Mol. Struct.* **1992**, *270*, 205–215. [[CrossRef](#)]
23. Grabowsky, S.; Hesse, M.F.; Paulmann, C.; Luger, P.; Beckmann, J. How to Make the Ionic Si–O Bond More Covalent and the Si–O–Si Linkage a Better Acceptor for Hydrogen Bonding. *Inorg. Chem.* **2009**, *48*, 4384–4393. [[CrossRef](#)] [[PubMed](#)]

24. Behr, J.P.; Dumas, P.; Moras, D. The  $\text{H}_3\text{O}^+$  Cation: Molecular Structure of an Oxonium-Macrocyclic Polyether Complex. *J. Am. Chem. Soc.* **1982**, *104*, 4540–4543. [[CrossRef](#)]
25. Atwood, J.L.; Bott, S.G.; Means, C.M.; Coleman, A.W.; Zhang, H.; May, M.T. Synthesis of salts of the hydrogen dichloride anion in aromatic solvents. 2. Syntheses and crystal structures of  $[\text{K}\cdot 18\text{-crown-6}][\text{Cl-H-Cl}]$ ,  $[\text{Mg}\cdot 18\text{-crown-6}][\text{Cl-H-Cl}]_2$ ,  $[\text{H}_3\text{O}\cdot 18\text{-crown-6}][\text{Cl-H-Cl}]$ , and the Related  $[\text{H}_3\text{O}\cdot 18\text{-crown-6}][\text{Br-H-Br}]$ . *Inorg. Chem.* **1990**, *29*, 467–470. [[CrossRef](#)]
26. Atwood, J.L.; Bott, S.G.; Robinson, K.D.; Bishop, E.J.; May, M.T. Preparation and X-ray structure of  $[\text{H}_3\text{O}^+ \cdot 18\text{-crown-6}][(\text{H}_5\text{O}_2^+)(\text{Cl}^-)_2]$ , a compound containing both  $\text{H}_3\text{O}^+$  and  $\text{H}_5\text{O}_2^+$  crystallized from aromatic solution. *J. Crystallogr. Spectrosc. Res.* **1991**, *21*, 459–462. [[CrossRef](#)]
27. Atwood, J.L.; Junk, P.C.; May, M.T.; Robinson, K.D. Synthesis and X-ray structure of  $[\text{H}_3\text{O}^+ \cdot 18\text{-crown-6}][\text{Br-Br-Br}^-]$ ; a compound containing both  $\text{H}_3\text{O}^+$  and a linear and symmetrical  $\text{Br}_3^-$  ion crystallized from aromatic solution. *J. Chem. Crystallogr.* **1994**, *24*, 243–245. [[CrossRef](#)]
28. Saleh, M.I.; Kusriani, E.; Fun, H.-K.; Teh, J.B.-J. Dicyclohexano-18-crown-6 hydroxonium tribromide. *Acta Cryst.* **2007**, *E63*, o3790–o3791. [[CrossRef](#)]
29. Kloo, L.; Svensson, P.H.; Taylor, M.J. Investigations of the polyiodides  $\text{H}_3\text{O}\cdot\text{I}_x$  ( $x = 3, 5$  or  $7$ ) as dibenzo-18-crown-6 complexes. *J. Chem. Soc. Dalton Trans.* **2000**, 1061–1065. [[CrossRef](#)]
30. Cheng, M.; Liu, X.; Luo, Q.; Duan, X.; Pei, C. Cocrystals of ammonium perchlorate with a series of crown ethers: Preparation, structures, and properties. *CrystEngComm* **2016**, *18*, 8487–8496. [[CrossRef](#)]
31. Feinberg, H.; Columbus, I.; Cohen, S.; Rabinovitz, M.; Shoham, G.; Selig, H. Crystallographic evidence for different modes of interaction of  $\text{BF}_3/\text{BF}_4^-$  species with water molecules and 18-crown-6. *Polyhedron* **1993**, *12*, 2913–2919. [[CrossRef](#)]
32. Dapporto, P.; Paoli, P.; Matijašić, I.; Tušek-Božić, L. Crystal structures of complexes of ammonium and potassium hexafluorophosphate with dibenzo-18-crown-6. Molecular mechanics studies on the uncomplexed macrocycle. *Inorg. Chim. Acta* **1996**, *252*, 383–389. [[CrossRef](#)]
33. Ponomarova, V.V.; Rusanova, J.A.; Rusanov, E.B.; Domasevitch, K.V. Unusual centrosymmetric structure of  $[\text{M}(18\text{-crown-6})]^+$  ( $\text{M} = \text{Rb}, \text{Cs}$  and  $\text{NH}_4$ ) complexes stabilized in an environment of hexachloridoantimonate(V) anions. *Acta Crystallogr. Sect. C Struct. Chem.* **2015**, *71*, 867–872. [[CrossRef](#)] [[PubMed](#)]
34. Hurd, D.T. On the Mechanism of the Acid-catalyzed Rearrangement of Siloxane Linkages in Organopolysiloxanes. *J. Am. Chem. Soc.* **1955**, *77*, 2998–3001. [[CrossRef](#)]
35. Cypryk, M.; Apeloig, Y. Mechanism of the Acid-Catalyzed Si–O Bond Cleavage in Siloxanes and Siloxanols. A Theoretical Study. *Organometallics* **2002**, *21*, 2165–2175. [[CrossRef](#)]
36. Wu, D.H.; Wu, Q.Q. Ammonium hexafluoridophosphate-18-crown-6 (1/1). *Acta Crystallogr. Sect. E Struct. Rep. Online* **2010**, *66*, 2–9. [[CrossRef](#)] [[PubMed](#)]
37. Shephard, D.S.; Zhou, W.; Maschmeyer, T.; Matters, J.M.; Roper, C.L.; Parsons, S.; Johnson, B.F.G.; Duer, M.J. Ortsspezifische Derivatisierung von MCM-41: Molekulare Erkennung und Lokalisierung funktioneller Gruppen in mesoporösen Materialien durch hochauflösende Transmissionselektronenmikroskopie. *Angew. Chem.* **1998**, *110*, 2847–2851. [[CrossRef](#)]
38. Kociok-Köhn, G.; Molloy, K.C.; Price, G.J.; Smith, D.R.G. Structural characterisation of trimethylsilyl-protected DNA bases. *Supramol. Chem.* **2008**, *20*, 697–707. [[CrossRef](#)]
39. Ha, H.-J.; Choi, C.-J.; Ahn, Y.-G.; Yun, H.; Dong, Y.; Lee, W.K. Cycloaddition of Lewis Acid-Induced *N*-Methylenylanilines as Azadienes to 1,2-Bistrimethylsilyloxycyclobutene and Oxidative Ring Expansion to 1,2,4,5-Tetrahydro-1-benzazocine-3,6-diones. *J. Org. Chem.* **2000**, *65*, 8384–8386. [[CrossRef](#)] [[PubMed](#)]
40. Becker, B.; Baranowska, K.; Chojnacki, J.; Wojnowski, W. Cubane-like structure of a silanethiol—Primary amine assembly—A novel, unusual hydrogen bond pattern. *Chem. Commun.* **2004**, 620–621. [[CrossRef](#)] [[PubMed](#)]
41. Polishchuk, A.P.; Makarova, N.N.; Astapova, T.V. X-ray diffraction investigation of *trans*-2,8-dihydroxy-2,8-diphenyl-4,4',6,6',10,10', 12,12'-octamethylcyclohexasiloxane and *trans*-2,8-dihydroxy-2,4,4',6,6',8,10,10', 12,12'-decamethyl-5-carbahexacyclosiloxane. *Crystallogr. Rep.* **2002**, *47*, 798–804. [[CrossRef](#)]
42. Spielberger, A.; Gspaltl, P.; Siegl, H.; Hengge, E.; Gruber, K. Syntheses, structures and properties of dihydroxypermethylcyclosilanes and permethylloxahexasilanorbornanes. *J. Organomet. Chem.* **1995**, *499*, 241–246. [[CrossRef](#)]

43. Driver, T.G.; Franz, A.K.; Woerpel, K.A. Diastereoselective Silacyclopropanations of Functionalized Chiral Alkenes. *J. Am. Chem. Soc.* **2002**, *124*, 6524–6525. [[CrossRef](#)] [[PubMed](#)]
44. Myers, A.G.; Dragovich, P.S. A Reaction Cascade Leading to 1,6-didehydro[10]annulene → 1,5-dehydronaphthalene Cyclization Initiated by Thiol Addition. *J. Am. Chem. Soc.* **1993**, *115*, 7021–7022. [[CrossRef](#)]
45. Veith, M.; Rammo, A. Synthese und Struktur eines neuartigen molekularen  $\lambda^5$ -Organospirosilikats und dessen dynamisches Verhalten in Lösung. *J. Organomet. Chem.* **1996**, *521*, 429–433. [[CrossRef](#)]
46. Heyns, A.M.; van Schalkwyk, G.J. A study of the infrared and Raman spectra of ammonium hexafluorophosphate  $\text{NH}_4\text{PF}_6$  over a wide range of temperatures. *Spectrochim. Acta Part A Mol. Spectrosc.* **1973**, *29*, 1163–1175. [[CrossRef](#)]
47. Willcott, M.R. MestRe Nova. *J. Am. Chem. Soc.* **2009**, *131*, 13180. [[CrossRef](#)]
48. OPUS; Version 7.2; Bruker Opt. GmbH: Ettlingen, Germany, 2012.
49. Sheldrick, G.M. SHELXT—Integrated space-group and crystal-structure determination. *Acta Crystallogr. Sect. A Found. Adv.* **2015**, *71*, 3–8. [[CrossRef](#)] [[PubMed](#)]
50. Sheldrick, G.M. Crystal structure refinement with SHELXL. *Acta Crystallogr. Sect. C Struct. Chem.* **2015**, *71*, 3–8. [[CrossRef](#)] [[PubMed](#)]
51. Dolomanov, O.V.; Bourhis, L.J.; Gildea, R.J.; Howard, J.A.K.; Puschmann, H. OLEX2: A complete structure solution, refinement and analysis program. *J. Appl. Crystallogr.* **2009**, *42*, 339–341. [[CrossRef](#)]
52. Diamond; Version 4.4.1; Crystal and Molecular Structure Visualization; Putz, H. & Brandenburg, K. GbR: Bonn, Germany, 2017.



© 2018 by the authors. Licensee MDPI, Basel, Switzerland. This article is an open access article distributed under the terms and conditions of the Creative Commons Attribution (CC BY) license (<http://creativecommons.org/licenses/by/4.0/>).